

# Learning Representational Invariances for Data-Efficient Action Recognition

Yuliang Zou<sup>1\*</sup>, Jinwoo Choi<sup>2\*</sup>, Qitong Wang<sup>1</sup>, Jia-Bin Huang<sup>1</sup>

<sup>1</sup>Virginia Tech <sup>2</sup>Kyung Hee University

\* indicates equal contribution

<https://yuliang.vision/video-data-aug>

## Abstract

*Data augmentation is a ubiquitous technique for improving image classification when labeled data is scarce. Constraining the model predictions to be invariant to diverse data augmentations effectively injects the desired representational invariances to the model (e.g., invariance to photometric variations), leading to improved accuracy. Compared to image data, the appearance variations in videos are far more complex due to the additional temporal dimension. Yet, data augmentation methods for videos remain under-explored. In this paper, we investigate various data augmentation strategies that capture different video invariances, including photometric, geometric, temporal, and actor/scene augmentations. When integrated with existing consistency-based semi-supervised learning frameworks, we show that our data augmentation strategy leads to promising performance on the Kinetics-100, UCF-101, and HMDB-51 datasets in the low-label regime. We also validate our data augmentation strategy in the fully supervised setting and demonstrate improved performance.*

## 1. Introduction

Deep neural networks have shown rapid progress in video action recognition [5, 13, 14, 38, 46, 53, 62, 64]. However, these approaches rely on training a model on a massive amount of *labeled* videos. For example, the Slow-Fast networks [14], R(2+1)D [53], I3D [5] are pre-trained on the Kinetics dataset [28], which contains  $300K \sim 650K$  manually labeled and temporally trimmed videos. The dependency on large-scale annotated video datasets is not scalable because manual labeling of videos is expensive, time-consuming, and error-prone. Hence, it is of great interest to investigate new approaches to improve data efficiency.

Data augmentation is a simple yet effective approach for improving data efficiency. Early work uses simple/weak augmentations to generate additional *realistic-looking* samples by applying geometric transformations (e.g. random scaling and cropping). Such approaches have

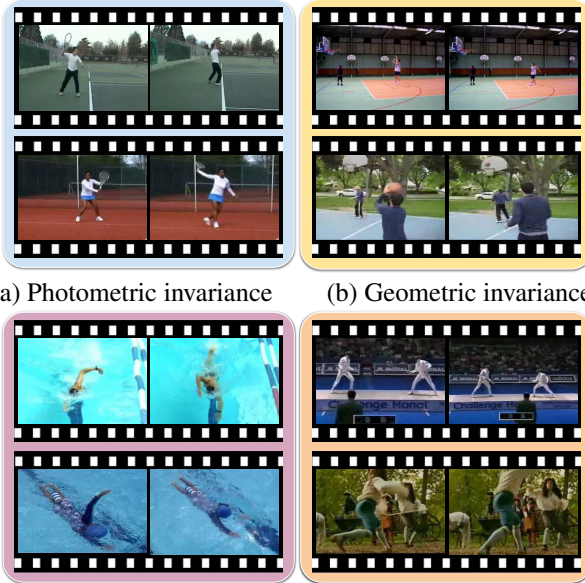


**Figure 1. Representative invariances for video action recognition.** Humans recognize actions in videos effortlessly, even in the presence of large photometric, geometric, temporal, and scene variations. Injecting these task-specific video invariances through data augmentations helps improve the data efficiency of video action recognition models. For each shaded block, we show two example videos of the *same* action, *i.e.* “Tennis swing”, “Basketball”, “Front Crawl”, and “Fencing”.

been widely used in training supervised image classification models [24, 26, 30]. While many realistic-looking visual examples are generated, these *weak* augmentations are ineffective in increasing the training data diversity because the augmented samples remain highly similar to the original ones. Recently, diverse/strong augmentations have been proposed [9, 10, 37]. By applying aggressive photometric and geometric transformations to the original data, strong augmentations help generate diverse training data and improve model performance in the supervised learning setting. Later, strong data augmentations have also shown their potential in consistency-based semi-supervised learn-

ing frameworks [49, 61]. The intuition behind the success of strong data augmentations in supervised and semi-supervised settings lies in learning *representational invariances* via regularizing a model to generate consistent predictions for diverse augmented views of the same data.

In this paper, we investigate and study strong data augmentation. While strong data augmentation in the image domain has been extensively studied [9, 10, 11, 37, 66], data augmentation techniques for videos remain under-explored. Recent self-supervised video representation learning approaches [19, 20, 42, 54, 55, 63] show the benefits of leverage some specific video invariances (*i.e.* spatial, temporal, etc.). However, each of these approaches only utilizes partial aspects of the desired representation invariances. In contrast, we provide a complete study in both semi-supervised and fully-supervised settings. As shown in Figure 1, we explore the following invariances: *photometric (color)*, *geometric (spatial)*, *temporal*, *scene (background)*, and investigate the corresponding data augmentation strategies that encourage the model learning these invariances.

Our results show that all these augmentation techniques help improve performance. With all the augmentations (as shown in Figure 2), we achieve favorable results on the Kinetics-100 [27], UCF-101 [50], and HMDB-51 [31] datasets in both low-label and full-label settings.

To summarize, we make the following contributions.

- We study various types of strong video data augmentation strategies for data-efficient action recognition.
- We introduce a novel scene augmentation strategy, ActorCutMix, to encourage the scene invariance.
- Our strong data augmentation strategies significantly improve the data efficiency in both the semi-supervised and fully-supervised learning settings, achieving promising results in standard video action recognition benchmarks.

## 2. Related Work

**Video recognition models.** Recent advances in video recognition focus on improving the network architecture design (*e.g.*, two-stream networks [15, 46], 3D CNNs [5, 21, 52, 56], 2D and 1D separable CNNs [53, 62], incorporating long-term temporal contexts [14, 56, 58]), and training efficiency [59]. Our focus in this work lies in improving *data efficiency* of video action classification by exploring data augmentation strategies from various perspectives: photometric, geometric, temporal, and actor/scene.

**Data augmentation.** Data augmentation is an essential component in modern deep neural network training. Early approaches [33, 43] only apply weak augmentations such as random translation and cropping. In addi-

tion to simple geometric transformations, random Gaussian, Dropout noise [1] and adversarial noise [40] have also been proposed for semi-supervised learning, leading to improved performance. Learning-based data augmentation approaches [9, 37] aim to avoid the manual design of data transformations. Such networks learn to adjust the data augmentation policy according to the feedback on a held-out (labeled) validation set. In supervised classification, recent methods [49, 61] apply strong image space augmentations (*e.g.*, RandAugment [10]) by cascading color jittering, geometric transformations, and regional dropout [11, 66], achieving state-of-the-art performance. Instead of perturbing the unlabeled images in the pixel space, several approaches [32, 57] propose to augment training examples in the feature space to complement conventional image space augmentations, providing further improvement. Most existing works design the data augmentation strategy specifically for *images*. In this work, we study data augmentation for *video* action recognition.

**Semi-supervised learning.** Semi-supervised learning (SSL) improves the performance using the abundant unlabeled data, alleviating the need for manual annotations. Most recent SSL approaches adopt either one of the following two strategies: (1) consistency regularization [32, 33, 40, 43, 51, 61], and (2) entropy minimization [18, 34]. The key insight of consistency regularization is that a model should generate *consistent* predictions for the same (unlabeled) data undergone different transformations/perturbations. Recently, holistic approaches [3, 4, 49, 61] that combine both the SSL strategies (consistency and entropy minimization) have been proposed to tackle the semi-supervised image classification task effectively. The consistency regularization within these SSL frameworks effectively encourages representational invariances to strongly-augmented views.

In the low-label settings, we leverage the FixMatch framework [49] to validate the efficacy of our video data augmentations. We also demonstrate improved results when integrating our augmentation strategies with another recent SSL framework, UDA [61].

Recently, Jing *et al.* [27] and Singh *et al.* [47] propose to adapt the SSL framework to the video domain. They focus on *algorithmic* improvement for video SSL. In contrast, our work complements these recent advances by exploring strong data augmentation strategies for videos.

**Self-supervised contrastive learning.** Recently, contrastive learning has emerged as a powerful tool for learning visual representations [6, 7, 22, 41, 44, 60]. In contrastive learning, a model learns representations by instance discrimination. These methods encourage feature embeddings from different augmentations of the same data to be similar, and feature embeddings from different data instances to be dissimilar to each other. Contrastive learning can be

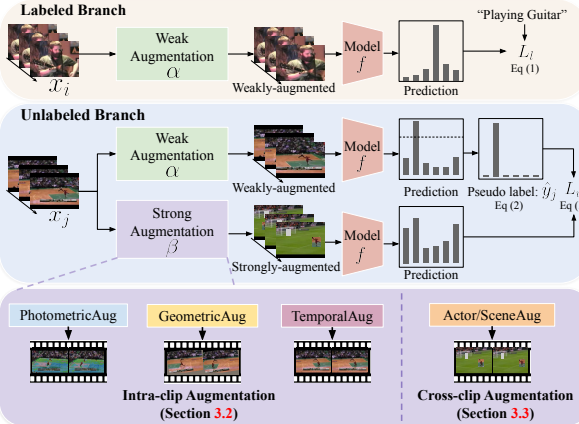


Figure 2. **Data-efficient action recognition.** In a low-label regime, we adopt the state-of-the-art semi-supervised learning framework [49] to validate the effectiveness of our explored strong data augmentation strategies. The overall training pipeline consists of (1) a labeled branch and (2) an unlabeled branch. We use ground truth labels to supervise the labeled branch. We use pseudo labels generated from weakly-augmented video clips to supervise the strongly-augmented counterpart in the unlabeled branch. Our contributions lie in the exploration of the *strong video augmentation*  $\beta$ .

viewed as injecting visual invariances. It pulls the representations of different augmented views of the same instance together, enforcing invariances to the selected data augmentations. Instead of injecting visual invariances in a self-supervised setting, we explore strong data augmentations in both semi-supervised and fully-supervised settings for video action recognition.

### 3. Video Data Augmentations

We explore strong and diverse video data augmentations mainly in the low-label setting. We formulate low-label video action recognition as a semi-supervised classification problem.

We first describe the semi-supervised classification formulation in Section 3.1. We then present our *intra-clip* data augmentation strategies (photometric, geometric, temporal) in Section 3.2. Next, we propose a *cross-clip* human-centric data augmentation operation, ActorCutMix, in Section 3.3. Lastly, we describe how we combine all these data augmentation operations to construct the final strong data augmentation strategy in Section 3.4.

#### 3.1. Semi-supervised learning

Considering a multi-class classification problem, we denote  $\mathcal{X} = \{(x_i, y_i)\}_{i=1}^{N_l}$  as the *labeled* training set, where  $x_i \in \mathcal{R}^{T \times H \times W \times 3}$  is the  $i$ -th sampled video clip,  $y_i$  is the corresponding one-hot ground truth label, and  $N_l$  is the number of data points in the labeled set. Similarly, we de-

note  $\mathcal{U} = \{x_j\}_{j=1}^{N_u}$  as the *unlabeled* set, where  $N_u$  is the number of data points in the unlabeled set. We use  $f_\theta$  to denote a classification model with trainable parameters  $\theta$ . We use  $\alpha(\cdot)$  to represent the weak (standard) augmentation (*i.e.*, random horizontal flip, random scaling, and random crop in video action recognition), and  $\beta(\cdot)$  to represent the *strong* data augmentation strategies (our focus).

We show an overview of the state-of-the-art semi-supervised classification pipeline [49] in Figure 2. We denote an input video clip consists of  $T$  frames as  $x_i$  throughout the paper. Given a mini-batch of *labeled* data  $\{(x_i, y_i)\}_{i=1}^{B_l}$ , we minimize the standard cross-entropy loss  $L_l$  defined as

$$L_l = -\frac{1}{B_l} \sum_{i=1}^{B_l} y_i \log f_\theta(\alpha(x_i)). \quad (1)$$

For a mini-batch of *unlabeled* data  $\{x_j\}_{j=1}^{B_u}$ , we enforce the model prediction consistency. More specifically, we generate pseudo-label  $\hat{y}$  for the unlabeled data via confidence thresholding

$$\mathcal{C} = \{x_j | \max f_\theta(\alpha(x_j)) \geq \tau\}, \quad (2)$$

where  $\tau$  denotes a pre-defined threshold and  $\mathcal{C}$  is the confident example set for the current mini-batch. We then convert the confident model predictions  $f_\theta(\alpha(x_j))$  to one-hot labels  $\hat{y}_j$  by taking *argmax* operation. We optimize a cross-entropy loss  $L_u$  for the confident set of unlabeled examples.

$$L_u = -\frac{1}{B_u} \sum_{x_j \in \mathcal{C}} \hat{y}_j \log f_\theta(\beta(x_j)). \quad (3)$$

Our overall training objective is the summation of (1) and (3).

$$L = L_l + \lambda_u L_u. \quad (4)$$

We set  $\lambda_u = 1$  and find it performs well empirically.

#### 3.2. Intra-clip data augmentation

**Temporally-coherent photometric and geometric augmentation.** Moderate photometric (color) and geometric (spatial) variations often do not affect the class semantics (*e.g.*, object classification). Thus, photometric and geometric augmentation strategies are widely used in supervised [10], self-supervised [6, 22], and semi-supervised [49] image classification tasks. Similar to image classification, videos from the same class also exhibit photometric (color) and geometric (spatial) variations (Figure 1(a-b)). It is thus natural to apply photometric and geometric data augmentation for video classification. However, as we validate with an ablation study in Section 4.2, individually applying state-of-the-art photometric and geometric augmentations

(e.g., RandAugment [10]) on each video frame leads to sub-optimal performance. We conjecture that the random transformations for each frame break the temporal coherency of a video clip. As a result, the frame-wise inconsistency within video clips may cause negative effects on the learned representations. A concurrent work [42] also validates the above assumption in the context of self-supervision video representation learning. Thus, we apply the same photometric and geometric transformations for every frame to maintain the temporal consistency within a sampled video clip. Specifically, we sample two basic operations from a pool of photometric and geometric transformations (as in RandAugment [10]) and then apply them to every frame for each video clip.

**Temporal augmentation.** In addition to color space and spatial dimension, there is a temporal dimension for videos. The additional temporal dimension significantly increases the variability of video data from many perspectives (e.g. speed, sampling rate, temporal order, etc.). To capture these task-specific representational invariances, we introduce three different types of temporal transformations: (1) T-Half, (2) T-Drop, and (3) T-Reverse, and we study the effect of these transformations. We illustrate the three temporal augmentations in Figure 3. First, to avoid a video recognition model focusing too much on particular frames instead of understanding the temporal context, we randomly drop some frames within a video clip. Randomly dropping frames is conceptually similar to the artificial occlusion augmentations, e.g. Cutout [11] operations in the spatial dimension in the image domain. We implement a temporal extension of Cutout in two ways: 1) We randomly discard the second half of a video clip and fill in the empty slots with the first half, referred to as T-Half. 2) For each frame in a video clip, we randomly replace it with its previous frame with a probability of  $p = 0.5$ , which we refer to as T-Drop. In addition to dropping part of the information, T-Drop also simulates *speeding-up* (frame indexes:  $[2, 3] \rightarrow [1, 3]$ ) and *slowing-down* (frame indexes:  $[1, 2] \rightarrow [1, 1]$  as shown in Figure 3) within a video clip. Such temporal augmentation regularizes the video classification model to generate consistent predictions for the two video clips (original and augmented ones) with different speed and temporal occlusion, implicitly encoding the speed/occlusion invariance. Second, we observe that many actions have periodic temporal structures and thus can be recognized no matter in the original chronological order or reverse. To capture this invariance of temporal order, we transform a video clip by reversing its temporal order, referred to as T-Reverse. As validated in the ablation study (Section 4.2), all three operations are beneficial for SSL video action recognition. Since these operations are complementary to each other, we put them in an operation pool (including the *identity* operation) and randomly sample one for each input video clip.

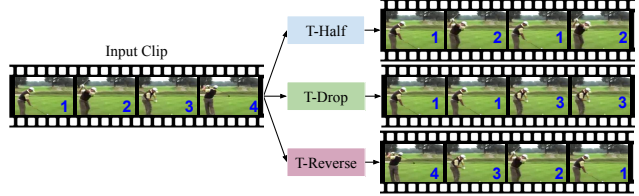


Figure 3. **Temporal augmentations.** We introduce three different temporal transformations: T-Half, T-Drop, and T-Reverse to achieve *temporal occlusion*, *speed*, and *order invariances*. Note that the **blue number** of each frame indicates the frame index within the corresponding video clip. We construct the final temporal augmentation by randomly selecting one of these transformed clips (including the original input) for each input video clip.

**Discussions.** By applying the aforementioned temporal augmentation, we encourage three types of temporal invariances during model training. (1) Invariance to partial temporal occlusion (T-Half and T-Drop): This invariance enforces models to recognize actions even with partial evidence. For example, humans can recognize the “Basketball” action by seeing only the first half (seeing bent arms with a ball, stretch arms but not seeing a ball flying). (2) Invariance to speed (T-Drop): The same action can be performed at a different speed. A model could also encounter videos containing the same actions but with different frame rates. Hence, encouraging action recognition models to be invariant to different speeds will be helpful. (3) Invariance to temporal (reverse) order (T-Reverse): For example, cyclic/order invariant actions such as “push/pull-ups”, “punching bags”, and many instrument-playing actions are invariant to reversed order. We observe that more than 50% of classes in standard human action recognition benchmarks are cyclic/order-invariant (e.g. 57 out of 101 in UCF-101 and 28 out of 51 in HMDB-51).

We validate the effectiveness of these temporal invariances in Table 1(b). Here, we discuss the limitation as well. First, for fine-grained action recognition [17, 39], a model may need to utilize the information from all the input frames to make a prediction. Also, speed difference may play a key role in discriminating the subtle differences between two similar actions (e.g. jogging v.s. running). Partial temporal occlusion invariance and speed invariance could hurt the overall performance in this case. Second, suppose we want to discriminate action classes with symmetric temporal orders (e.g. move an object from left to right v.s. move an object from right to left). In that case, encouraging temporal order invariance can be harmful. However, we find all three temporal invariances helpful for general coarse-grained human action recognition purposes, particularly in a low-label regime. Note that the users can always decide which temporal invariance to inject depending on the specific video tasks.

### 3.3. Cross-clip data augmentation

**ActorCutMix.** There are severe scene representation biases [8, 35, 36] in the popular action recognition datasets such as UCF-101, HMDB-51, Kinetics-400, Charades [45], and ActivityNet [12], *etc.* Action recognition models trained on these scene-biased datasets tend to leverage the background scene information instead of actual action. These scene-biased action recognition models are likely to fail when tested on the new data with unseen actor-scene combinations. For example, people can do “Fencing” both in a gym or in a forest, as shown in the scene invariance block in Figure 1(d). Training a model on the data consists of “Fencing” actions in gyms only will likely fail when tested on the new data consists of “Fencing” actions in forests. To mitigate the scene bias, we propose a new human-centric video data augmentation method, ActorCutMix. The operation of the proposed ActorCutMix is similar to CutMix [66] in mixing the pixels from different samples to create new training data. However, our method differs in motivation. ActorCutMix aims to improve *scene invariance*, regularizing a video classification model to focus on the actor to make predictions (*i.e.* scene debiasing). In contrast, the goal of CutMix is to achieve *occlusion robustness*, encouraging a model to make correct predictions even when part of the image input is occluded.

As shown in Figure 4, ActorCutMix generates new training examples  $(\tilde{x}_A, \tilde{y}_A)$ ,  $(\tilde{x}_B, \tilde{y}_B)$  by swapping the background regions in the two training examples  $(x_A, \hat{y}_A)$ , and  $(x_B, \hat{y}_B)$  in a mini-batch, where  $x$  is a video clip and  $\hat{y}$  is the corresponding pseudo-label. We define the swapping operation as follows:

$$\begin{aligned} \tilde{x}_A &= m_A \odot x_A + (\mathbf{1} - m_A) \odot (\mathbf{1} - m_B) \odot x_B, \\ \tilde{y}_A &= \lambda \hat{y}_A + (1 - \lambda) \hat{y}_B. \end{aligned} \quad (5)$$

Here,  $m \in \mathcal{R}^{T \times H \times W \times 3}$  is a binary human mask for a video clip, with a value of 1 for human regions and 0 for the background regions.  $\odot$  represents the element-wise multiplication.  $\lambda$  is a combination ratio for label smoothing. The other augmented training sample and its pseudo label  $(\tilde{x}_B, \tilde{y}_B)$  can be generated similarly. We generate the human mask  $m$  by running an off-the-shelf human detection algorithm [23] without fine-tuning on the video datasets. We run the human detector on the video datasets offline and load the cached human bounding boxes during training. We demonstrate that ActorCutMix significantly improves the semi-supervised action recognition performance in Section 4.2.

**Label smoothing.** A straightforward way to select the combination ratio  $\lambda$  in (5) is to set it according to the foreground mask ratio. Assume  $x_A \in \mathcal{R}^{T \times H \times W \times 3}$ , then we

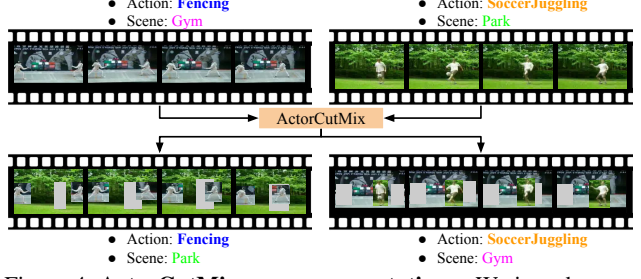


Figure 4. **ActorCutMix scene augmentation.** We introduce an actor/scene augmentation method for learning *scene invariance* in semi-supervised action recognition. Specifically, we transform two video clips by swapping the background regions of the video clips. We generate human/background masks by running an off-the-shelf human detector. We smooth labels to mitigate data corruption due to the missing/false-positive human detections.

can compute the foreground ratio

$$\gamma = \frac{\sum m_A}{THW}, \quad (6)$$

and then use  $\gamma$  as a combination ratio  $\lambda$  as in CutMix. We emphasize that ActorCutMix and CutMix have different purposes of label smoothing. The purpose of label smoothing in CutMix is to provide multiple labels for a single training image, as a training image consists of information from two different classes (*e.g.*, a dog and a cat). In contrast, we smooth labels in ActorCutMix to mitigate data corruption due to the missing/false-positive human detections. Ideally, suppose we have a perfect human detector. In this case, the pseudo label of the video clip  $x_A$  should be  $\tilde{y}_A = \hat{y}_A$ . In other words, we aim to recognize the *human action* instead of the background scene. However, due to missing/false-positive human detections, an augmented video clip could potentially contain humans performing different actions from different clips. Therefore, to prevent model confusion, we apply label smoothing with a higher weight for the label of the (potentially corrupted) human action  $\hat{y}_A$  and a lower weight for the label of the (potentially corrupted) background scene  $\hat{y}_B$ , via the following scaling function:

$$\lambda = -(\gamma - 1)^\alpha + 1, \gamma \in [0, 1] \quad (7)$$

where we empirically find  $\alpha = 4$  yields good results.

**Discussions.** By applying ActorCutMix, we are essentially injecting the scene invariance into the model, mitigating the reliance on the scene context. In other words, we encourage a model to recognize the action class by focusing on the actor, no matter what the background scene is. Indeed, we argue that scene context sometimes provides useful cues for recognizing the actions. However, deep neural networks tend to learn shortcuts [11, 16, 25, 48, 66] without proper regularization. A model could learn spurious corre-

---

**Algorithm 1:** Strong video data augmentation

---

**Input** : A mini-batch of unlabeled video clips  $X$  and the corresponding human mask  $M$

1 Draw a sample  $p$  from uniform distribution  $U(0, 1)$

2 **If**  $p > 0.5$

3   Reverse the order of the batch dimension to get  $X'$  and  $M'$

4    $\tilde{X}, \tilde{X}' = \text{ActorCutMix}(X, X', M, M')$

5 **else**

6   **for** each video clip  $x$  in  $X$

7     Sample  $op_1, op_2$  from photometric-geometric op pool,  $op_3$  from temporal op pool

8      $\tilde{x} = \text{PhotometricGeometricAug}(x, op_1, op_2)$

9      $\tilde{x} = \text{TemporalAug}(\tilde{x}, op_3)$

10   **end for**

11 **end if**

**Return:** Strongly-augmented video clips  $\tilde{X}$

---

lations between the action and the scene instead of focusing on the human action itself [2, 8], *i.e.* predicting the action class according to the scene context only. We regularize the network to focus on human actions by changing the background context.

Note that scene invariance also has its limitation. For example, if our goal is to discriminate different actions in the same background context (*e.g.* the Diving48 dataset [35]), ActorCutMix makes no difference. Also, the current combination of the actors and the scenes could cause visual artifacts that may be harmful as shown in other copy and paste-based augmentations [11, 29, 65, 66]. More accurate segmentation of the actors (and probably the objects) may further improve the performance. We leave it as a future direction.

### 3.4. Combining different data augmentations

Algorithm 1 outlines the combined strong augmentation.

**Combining photometric-geometric and temporal augmentations.** We combine the photometric-geometric and temporal augmentations by cascading both of them. This can be regarded as a spatial-temporal counterpart of RandAugment [10]: Randomly sample two operations from photometric and geometric augmentation operations, and then sample one operation from the temporal augmentation operations. We refer this combined augmentation as *intra-clip augmentation*.

**Combining intra-clip and cross-clip augmentations.** Now we have both intra-clip augmentation (photometric-geometric-temporal) and cross-clip augmentation (ActorCutMix). To combine these two very different augmentation strategies, we propose randomly applying either one of them for each mini-batch. We validate the effectiveness of

this combination in Section 4.2.

## 4. Experimental Results

### 4.1. Experimental setup

**Dataset.** We conduct experiments on the public action recognition benchmarks: UCF-101 [50], HMDB-51 [31], and Kinetics-100 [27, 28]. UCF-101 consists of 13,320 videos with 101 action classes. HMDB-51 consists of 6,766 videos with 51 action classes. The full Kinetics dataset consists of 300K videos with 400 classes. We use a subset, Kinetics-100, which consists of 90K videos with 100 classes. We split the datasets following Jing *et al.* [27] to conduct semi-supervised training based on the state-of-the-art FixMatch framework [49].

**Evaluation metrics.** For all the datasets, we report top-1 accuracy for quantitative comparison.

**Compared methods.** As a first baseline, we train a model with only the labeled data using standard/weak video data augmentations (*e.g.* random scaling, horizontal flipping, etc.). We call it as *supervised baseline*. In the low-label setting, we also compare our method with VideoSSL [27] and several semi-supervised methods adapted to video (*i.e.*, PseudoLabel [34], MeanTeacher [51], S4L [67]).

**Implementation details.** We implement our method on top of the publicly available mmaction2 codebase.<sup>1</sup> Unless specified, we use the R(2+1)D model [53] with ResNet-34 [24] as the feature extraction backbone. To better understand the effect of our augmentation techniques, we initialize the model with random weights (as opposed to using models with supervised pre-training on ImageNet or Kinetics). We sample eight frames from each video randomly and uniformly to construct a clip with an eight-frame sampling interval. For the supervised learning baseline, we use a batch size of 16 clips for each GPU. We use a mini-batch of five clips from labeled data and five clips from unlabeled data for each GPU for our semi-supervised learning method. We train our models using 8 RTX 2080 Ti GPUs. We provide more implementation details in the supplementary document.

### 4.2. Ablation study

We conduct ablation experiments on the 20% label split of the UCF-101 dataset [50] using a R(2+1)D ResNet-34 model in the semi-supervised learning setting based on FixMatch [49]. In the following, we validate each design choice of our strong data augmentation strategy.

**Temporally-coherent photometric-geometric augmentation.** We first conduct an ablation experiment to study the necessity of applying *temporally-coherent* photometric-geometric augmentation. As shown in Table 1(a), although

<sup>1</sup><https://github.com/open-mmlab/mmaction2>

Table 1. **Ablation study.** We conduct experiments with an R(2+1)D ResNet-34 model on the 20% label split of the UCF-101 dataset.

(a) Temporally-coherent photo.-geo. aug.

Strategy	Top-1 acc.
Supervised baseline	38.91
Per-frame	44.17
Temporally-coherent	<b>53.37</b>

(b) Temporal augmentation

Strategy	Top-1 acc.
T-Half	42.77
T-Drop	43.14
T-Reverse	43.40
TemporalAll	<b>44.07</b>

(c) ActorCutMix augmentation

Strategy	Top-1 acc.
Supervised baseline	38.91
w/o label smoothing	42.82
w/ label smoothing	<b>45.28</b>

(d) Combining intra-clip augs.

Strategy	Top-1 acc.
Supervised baseline	38.91
Randomly sample one	53.37
Cascaded	<b>54.48</b>

(e) Combining intra- and inter-clip augs.

Strategy	Top-1 acc.
Supervised baseline	38.91
Cascaded	50.89
Randomly sample one	<b>56.73</b>

(f) Different initialization

	Initialization	
	Random	Kinetics-400
Supervised	38.91	72.40
Ours	<b>56.73</b>	<b>77.37</b>

applying photometric-geometric augmentation individually in a frame-by-frame manner improves upon the supervised baseline ( $38.91\% \rightarrow 44.17\%$ ), using temporally-coherent augmentation further enhances the performance by a large margin ( $44.17\% \rightarrow 53.37\%$ ). The results validate our hypothesis that preserving frame-wise consistency in the augmented videos leads to improved results.

**Temporal augmentation.** Next, we study the effectiveness of temporal augmentation and its atomic operations. As shown in Table 1(b), all of the atomic operations are beneficial to the recognition accuracy. The results validate our motivation: Temporal occlusion, speed, and order invariances are beneficial for coarse-grained human action recognition, improving the data efficiency. With all the atomic temporal operations combined, the final temporal augmentation further improves the accuracy.

**ActorCutMix augmentation.** We validate the proposed human-centric data augmentation, ActorCutMix in Table 1(c). ActorCutMix shows moderate improvement over the baseline without label smoothing. With label smoothing, ActorCutMix shows even more significant performance improvement. The results validate that capturing scene invariance improves recognition accuracy. Our results suggest that label smoothing can mitigate data corruption caused by the missing/false-positive human detections.

**Combining photometric-geometric and temporal augmentations.** In this ablation experiment, we study how to combine photometric-geometric augmentation and temporal augmentation. We explore an alternative combination strategy: sample only one of them and apply it for a video clip. As shown in Table 1(d), our default cascaded strategy leads to better performance, indicating that combining photometric-geometric and temporal augmentations in a cascaded manner is more effective.

**Combining intra-clip and cross-clip augmentations.** Similarly, we study how to combine both intra-clip

(photometric-geometric-temporal) and cross-clip (ActorCutMix) data augmentations. A straightforward approach combines these two types of augmentations in a cascaded fashion, the same as intra-clip transformation combinations. Surprisingly, as shown in Table 1(e), we find that the cascaded data augmentation is even *worse* than applying the intra-clip augmentation alone. Our intuition is that cascading intra-clip and cross-clip augmentation produces severely distorted video clips that no longer resemble natural videos. Hence, we randomly apply only one data augmentation selected from intra-clip *or* cross-clip for each input video clip.

**Strong augmentation on the labeled branch.** Currently, the *strong* data augmentation is only applied to the unlabeled branch by default, as shown in Figure 2. Here, we conduct an experiment applying the strong augmentation on the labeled branch as well. It achieves a similar performance (56.46%) as our default setting (56.73%). We conjecture that the strong augmentations have already injected the visual invariances in the unlabeled branch. Additional strong augmentation for the labeled branch may not add more visual invariances to the model. Therefore, the performance difference is negligible. For better training efficiency, we choose to use the default setting.

**Different initialization.** Lastly, we aim to test if our strong data augmentation strategy can still improve over the *supervised baseline*, given strong pre-trained model weights as an initialization. As shown in Table 1(f), while the improvement over the supervised baseline is not as significant as the boost in the train-from-scratch setting, the proposed method can still achieve a sizable improvement ( $72.40\% \rightarrow 77.37\%$ ). The results validate the general applicability of the strong data augmentation in practical scenarios.

Table 2. **Comparison with the state of the arts.** All the methods use a 3D ResNet-18 model. The best performance is in **bold** and the second best is underlined.

Method	w/ ImageNet	Kinetics-100 20%	UCF-101				HMDB-51		
	distillation		50%	20%	10%	5%	60%	50%	40%
PseudoLabel [34]	-	48.0	47.5	37.0	24.7	17.6	33.5	32.4	27.3
MeanTeacher [51]	-	47.1	45.8	36.3	25.6	17.5	32.2	30.4	27.2
S4L [67]	-	51.1	47.9	37.7	29.1	22.7	35.6	31.0	29.8
VideoSSL [27]	✓	<u>57.7</u>	54.3	48.7	<b>42.0</b>	<b>32.4</b>	<u>37.0</u>	<u>36.2</u>	<u>32.7</u>
Ours	-	<b>61.2</b>	<b>59.9</b>	<b>51.7</b>	<u>40.2</u>	<u>27.0</u>	<b>38.9</b>	<b>38.2</b>	<b>32.9</b>

Table 3. **Improvement over different SSL frameworks.** Our strong data augmentation strategies can be integrated into different SSL methods. We show results from an R(2+1)D ResNet-34 model on the 20% label split of UCF-101.

	Semi-supervised framework	
	FixMatch [49]	UDA [61]
Strong data augmentation		
Per-frame photo.-geo.	44.17	43.11
Temporally-coherent photo.-geo.	53.37	50.20
Ours	<b>56.73</b>	<b>54.80</b>

### 4.3. Improvement over vanilla semi-supervised frameworks

We show that our strong data augmentation is method-agnostic. We plug our strong data augmentation into the unlabeled branches of two existing semi-supervised learning frameworks. We conduct experiments on the 20% label split of the UCF-101 dataset, using an R(2+1)D ResNet-34 model. As shown in Table 3, the per-frame augmentation baseline can be regarded as the vanilla version of these two semi-supervised learning frameworks. Using our strong data augmentation strategy constantly improves the performance by a large margin.

### 4.4. Comparing with the state of the arts

Next, we compare our method on several established benchmarks, following the same data splits as in Jing *et al.* [27].<sup>2</sup> As shown in Table 2, our method consistently achieves favorable performance compared with other approaches with the same amount of supervision. On the UCF-101 dataset, we observe that VideoSSL [27] achieves better performance in the extremely low label ratios (10% and 5%) than ours while being worse in other label ratios. We hypothesize that the ImageNet pre-trained model’s knowledge distillation plays a crucial role in the extremely low-label regime. The improvement from the distillation might become marginal quickly as the number of labeled data grows. Following VideoSSL [27], we incorporate the additional knowledge distillation supervision into our

<sup>2</sup>Due to our limited computing resources, we only conduct experiments under the 20% label ratio in the Kinetics-100 dataset.

Table 4. **Full-label setting.** Our strong data augmentation strategies outperform standard video data augmentation (*i.e.* random horizontal flipping, scaling, cropping) in the fully-supervised training setting using all the labeled examples as well. We train R(2+1)D ResNet-34 models from scratch for the experiments.

Augmentation	Dataset	
	UCF-101	HMDB-51
Standard	55.67	40.78
Ours	<b>68.31</b>	<b>44.51</b>

model in the extremely low-label ratio experiments. We find that it complements our strong data augmentation, further improving our method to achieve the state-of-the-art (53.0% in 10% split and 45.1% in 5% split of UCF-101). We include full results and the comparisons with two recent self-supervised methods in the supplementary document.

### 4.5. Full-label setting results

Lastly, we show that the proposed strong data augmentation can further improve supervised training in the full-label setting. We train an R(2+1)D ResNet-34 model from scratch and replace the standard weak video augmentation operations (*i.e.* random horizontal flip, scaling, cropping) with our strong data augmentation strategy in Algorithm 1. As shown in Table 4, applying our strong augmentation leads to a significant performance boost on both the UCF-101 (55.67%  $\rightarrow$  68.31%) and HMDB-51 (40.78%  $\rightarrow$  44.51%) datasets.

## 5. Conclusions

In this paper, we investigate different types of data augmentation strategies for video action recognition, in both low-label and full-label settings. Our study shows the importance of (1) temporally-coherent photometric and geometric augmentations, (2) temporal augmentations, and (3) actor/scene augmentation. We show promising action recognition performance on the public benchmarks in both low-label and full-label settings with all the augmentations. We believe that our exploration help facilitates future video action recognition research.

## References

- [1] Philip Bachman, Ouais Alsharif, and Doina Precup. Learning with pseudo-ensembles. In *NeurIPS*, 2014. 2
- [2] Hyojin Bahng, Sanghyuk Chun, Sangdoo Yun, Jaegul Choo, and Seong Joon Oh. Learning de-biased representations with biased representations. In *ICML*, 2020. 6
- [3] David Berthelot, Nicholas Carlini, Ekin D Cubuk, Alex Kurakin, Kihyuk Sohn, Han Zhang, and Colin Raffel. Remixmatch: Semi-supervised learning with distribution matching and augmentation anchoring. In *ICLR*, 2020. 2
- [4] David Berthelot, Nicholas Carlini, Ian Goodfellow, Nicolas Papernot, Avital Oliver, and Colin A Raffel. Mixmatch: A holistic approach to semi-supervised learning. In *NeurIPS*, 2019. 2
- [5] Joao Carreira and Andrew Zisserman. Quo vadis, action recognition? a new model and the kinetics dataset. In *CVPR*, 2017. 1, 2
- [6] Ting Chen, Simon Kornblith, Mohammad Norouzi, and Geoffrey Hinton. A simple framework for contrastive learning of visual representations. In *ICML*, 2020. 2, 3
- [7] Xinlei Chen, Haoqi Fan, Ross Girshick, and Kaiming He. Improved baselines with momentum contrastive learning. *arXiv preprint arXiv:2003.04297*, 2020. 2
- [8] Jinwoo Choi, Chen Gao, Joseph CE Messou, and Jia-Bin Huang. Why can't i dance in the mall? learning to mitigate scene bias in action recognition. In *NeurIPS*, 2019. 5, 6
- [9] Ekin D Cubuk, Barret Zoph, Dandelion Mane, Vijay Vasudevan, and Quoc V Le. Autoaugment: Learning augmentation policies from data. In *CVPR*, 2019. 1, 2
- [10] Ekin D Cubuk, Barret Zoph, Jonathon Shlens, and Quoc V Le. Randaugment: Practical automated data augmentation with a reduced search space. In *CVPR Workshops*, 2020. 1, 2, 3, 4, 6
- [11] Terrance DeVries and Graham W Taylor. Improved regularization of convolutional neural networks with cutout. *arXiv preprint arXiv:1708.04552*, 2017. 2, 4, 5, 6
- [12] Bernard Ghanem, Fabian Caba Heilbron, Victor Escorcia and Juan Carlos Niebles. Activitynet: A large-scale video benchmark for human activity understanding. In *CVPR*, 2015. 5
- [13] Christoph Feichtenhofer. X3d: Expanding architectures for efficient video recognition. In *CVPR*, 2020. 1
- [14] Christoph Feichtenhofer, Haoqi Fan, Jitendra Malik, and Kaiming He. Slowfast networks for video recognition. In *ICCV*, 2019. 1, 2
- [15] Christoph Feichtenhofer, Axel Pinz, and Andrew Zisserman. Convolutional two-stream network fusion for video action recognition. In *CVPR*, 2016. 2
- [16] Robert Geirhos, Patricia Rubisch, Claudio Michaelis, Matthias Bethge, Felix A Wichmann, and Wieland Brendel. Imagenet-trained cnns are biased towards texture; increasing shape bias improves accuracy and robustness. In *ICLR*, 2018. 5
- [17] Raghav Goyal, Samira Ebrahimi Kahou, Vincent Michalski, Joanna Materzynska, Susanne Westphal, Heuna Kim, Valentin Haenel, Ingo Fruend, Peter Yianilos, Moritz Mueller-Freitag, et al. The " something something" video database for learning and evaluating visual common sense. In *ICCV*, 2017. 4
- [18] Yves Grandvalet and Yoshua Bengio. Semi-supervised learning by entropy minimization. In *NeurIPS*, 2005. 2
- [19] Tengda Han, Weidi Xie, and Andrew Zisserman. Video representation learning by dense predictive coding. In *ICCV Workshops*, 2019. 2
- [20] Tengda Han, Weidi Xie, and Andrew Zisserman. Memory-augmented dense predictive coding for video representation learning. In *ECCV*, 2020. 2
- [21] Kensho Hara, Hirokatsu Kataoka, and Yutaka Satoh. Can spatiotemporal 3d cnns retrace the history of 2d cnns and imagenet? In *CVPR*, 2018. 2
- [22] Kaiming He, Haoqi Fan, Yuxin Wu, Saining Xie, and Ross Girshick. Momentum contrast for unsupervised visual representation learning. In *CVPR*, 2020. 2, 3
- [23] Kaiming He, Georgia Gkioxari, Piotr Dollár, and Ross Girshick. Mask R-CNN. In *ICCV*, 2017. 5
- [24] Kaiming He, Xiangyu Zhang, Shaoqing Ren, and Jian Sun. Deep residual learning for image recognition. In *CVPR*, 2016. 1, 6
- [25] Lisa Anne Hendricks, Kaylee Burns, Kate Saenko, Trevor Darrell, and Anna Rohrbach. Women also snowboard: Overcoming bias in captioning models. In *ECCV*, 2018. 5
- [26] Gao Huang, Zhuang Liu, Laurens Van Der Maaten, and Kilian Q Weinberger. Densely connected convolutional networks. In *CVPR*, 2017. 1
- [27] Longlong Jing, Toufiq Parag, Zhe Wu, Yingli Tian, and Hongcheng Wang. Videossal: Semi-supervised learning for video classification. In *WACV*, 2021. 2, 6, 8
- [28] Will Kay, Joao Carreira, Karen Simonyan, Brian Zhang, Chloe Hillier, Sudheendra Vijayanarasimhan, Fabio Viola, Tim Green, Trevor Back, Paul Natsev, et al. The kinetics human action video dataset. *arXiv preprint arXiv:1705.06950*, 2017. 1, 6
- [29] Jang-Hyun Kim, Wonho Choo, and Hyun Oh Song. Puzzle mix: Exploiting saliency and local statistics for optimal mixup. In *ICML*, 2020. 6
- [30] Alex Krizhevsky, Ilya Sutskever, and Geoffrey E Hinton. Imagenet classification with deep convolutional neural networks. In *NeurIPS*, 2012. 1
- [31] Hildegarde Kuehne, Hueihan Jhuang, Estibaliz Garrote, Tomaso Poggio, and Thomas Serre. HMDB: A large video database for human motion recognition. In *ICCV*, 2011. 2, 6
- [32] Chia-Wen Kuo, Chih-Yao Ma, Jia-Bin Huang, and Zsolt Kira. Featmatch: Feature-based augmentation for semi-supervised learning. In *ECCV*, 2020. 2
- [33] Samuli Laine and Timo Aila. Temporal ensembling for semi-supervised learning. In *ICLR*, 2016. 2
- [34] Dong-Hyun Lee. Pseudo-label: The simple and efficient semi-supervised learning method for deep neural networks. In *ICML Workshop*, 2013. 2, 6, 8
- [35] Yingwei Li, Yi Li, and Nuno Vasconcelos. Resound: Towards action recognition without representation bias. In *ECCV*, 2018. 5, 6

[36] Yi Li and Nuno Vasconcelos. Repair: Removing representation bias by dataset resampling. In *CVPR*, 2019. 5

[37] Sungbin Lim, Ildoo Kim, Taesup Kim, Chiheon Kim, and Sungwoong Kim. Fast autoaugment. In *NeurIPS*, 2019. 1, 2

[38] Ji Lin, Chuang Gan, and Song Han. Tsm: Temporal shift module for efficient video understanding. In *ICCV*, 2019. 1

[39] Farzaneh Mahdisoltani, Guillaume Berger, Waseem Gharbieh, David Fleet, and Roland Memisevic. On the effectiveness of task granularity for transfer learning. *arXiv preprint arXiv:1804.09235*, 2018. 4

[40] Takeru Miyato, Shin-ichi Maeda, Masanori Koyama, and Shin Ishii. Virtual adversarial training: a regularization method for supervised and semi-supervised learning. *TPAMI*, 41(8):1979–1993, 2018. 2

[41] Senthil Purushwalkam and Abhinav Gupta. Demystifying contrastive self-supervised learning: Invariances, augmentations and dataset biases. In *NeurIPS*, 2020. 2

[42] Rui Qian, Tianjian Meng, Boqing Gong, Ming-Hsuan Yang, Huiheng Wang, Serge Belongie, and Yin Cui. Spatiotemporal contrastive video representation learning. In *CVPR*, 2021. 2, 4

[43] Mehdi Sajjadi, Mehran Javanmardi, and Tolga Tasdizen. Regularization with stochastic transformations and perturbations for deep semi-supervised learning. In *NeurIPS*, 2016. 2

[44] Pierre Sermanet, Corey Lynch, Yevgen Chebotar, Jasmine Hsu, Eric Jang, Stefan Schaal, Sergey Levine, and Google Brain. Time-contrastive networks: Self-supervised learning from video. In *ICRA*, 2018. 2

[45] Gunnar A Sigurdsson, Gü̈l Varol, Xiaolong Wang, Ali Farhadi, Ivan Laptev, and Abhinav Gupta. Hollywood in homes: Crowdsourcing data collection for activity understanding. In *ECCV*, 2016. 5

[46] Karen Simonyan and Andrew Zisserman. Two-stream convolutional networks for action recognition in videos. In *NeurIPS*, 2014. 1, 2

[47] Ankit Singh, Omprakash Chakraborty, Ashutosh Varshney, Rameswar Panda, Rogerio Feris, Kate Saenko, and Abir Das. Semi-supervised action recognition with temporal contrastive learning. *arXiv preprint arXiv:2102.02751*, 2021. 2

[48] Krishna Kumar Singh and Yong Jae Lee. Hide-and-seek: Forcing a network to be meticulous for weakly-supervised object and action localization. In *ICCV*, 2017. 5

[49] Kihyuk Sohn, David Berthelot, Chun-Liang Li, Zizhao Zhang, Nicholas Carlini, Ekin D Cubuk, Alex Kurakin, Han Zhang, and Colin Raffel. Fixmatch: Simplifying semi-supervised learning with consistency and confidence. In *NeurIPS*, 2020. 2, 3, 6, 8

[50] Khurram Soomro, Amir Roshan Zamir, and Mubarak Shah. UCF101: A dataset of 101 human actions classes from videos in the wild. *arXiv preprint arXiv:1212.0402*, 2012. 2, 6

[51] Antti Tarvainen and Harri Valpola. Mean teachers are better role models: Weight-averaged consistency targets improve semi-supervised deep learning results. In *NeurIPS*, 2017. 2, 6, 8

[52] Du Tran, Lubomir Bourdev, Rob Fergus, Lorenzo Torresani, and Manohar Paluri. Learning spatiotemporal features with 3d convolutional networks. In *ICCV*, 2015. 2

[53] Du Tran, Heng Wang, Lorenzo Torresani, Jamie Ray, Yann LeCun, and Manohar Paluri. A closer look at spatiotemporal convolutions for action recognition. In *CVPR*, 2017. 1, 2, 6

[54] Michael Tschannen, Josip Djolonga, Marvin Ritter, Aravindh Mahendran, Neil Houlsby, Sylvain Gelly, and Mario Lucic. Self-supervised learning of video-induced visual invariances. *arXiv preprint arXiv:1912.02783*, 2019. 2

[55] Jiangliu Wang, Jianbo Jiao, and Yun-Hui Liu. Self-supervised video representation learning by pace prediction. In *ECCV*, 2020. 2

[56] Xiaolong Wang, Ross Girshick, Abhinav Gupta, and Kaiming He. Non-local neural networks. In *CVPR*, 2018. 2

[57] Yulin Wang, Gao Huang, Shiji Song, Xuran Pan, Yitong Xia, and Cheng Wu. Regularizing deep networks with semantic data augmentation. *arXiv preprint arXiv:2007.10538*, 2020. 2

[58] Chao-Yuan Wu, Christoph Feichtenhofer, Haoqi Fan, Kaiming He, Philipp Krahenbuhl, and Ross Girshick. Long-term feature banks for detailed video understanding. In *CVPR*, 2019. 2

[59] Chao-Yuan Wu, Ross Girshick, Kaiming He, Christoph Feichtenhofer, and Philipp Krahenbuhl. A multigrid method for efficiently training video models. In *CVPR*, 2020. 2

[60] Tete Xiao, Xiaolong Wang, Alexei A Efros, and Trevor Darrell. What should not be contrastive in contrastive learning. In *ICLR*, 2021. 2

[61] Qizhe Xie, Zihang Dai, Eduard Hovy, Minh-Thang Luong, and Quoc V Le. Unsupervised data augmentation for consistency training. In *NeurIPS*, 2020. 2, 8

[62] Saining Xie, Chen Sun, Jonathan Huang, Zhuowen Tu, and Kevin Murphy. Rethinking spatiotemporal feature learning for video understanding. In *ECCV*, 2018. 1, 2

[63] Dejing Xu, Jun Xiao, Zhou Zhao, Jian Shao, Di Xie, and Yueteng Zhuang. Self-supervised spatiotemporal learning via video clip order prediction. In *CVPR*, 2019. 2

[64] Ceyuan Yang, Yinghao Xu, Jianping Shi, Bo Dai, and Bolei Zhou. Temporal pyramid network for action recognition. In *CVPR*, 2020. 1

[65] Jaejun Yoo, Namhyuk Ahn, and Kyung-Ah Sohn. Rethinking data augmentation for image super-resolution: A comprehensive analysis and a new strategy. In *CVPR*, 2020. 6

[66] Sangdoo Yun, Dongyoon Han, Seong Joon Oh, Sanghyuk Chun, Junsuk Choe, and Youngjoon Yoo. Cutmix: Regularization strategy to train strong classifiers with localizable features. In *ICCV*, 2019. 2, 5, 6

[67] Xiaohua Zhai, Avital Oliver, Alexander Kolesnikov, and Lucas Beyer. S4l: Self-supervised semi-supervised learning. In *ICCV*, 2019. 6, 8